ON THE DECORRELATION EFFECT OF DRY SNOW IN DIFFERENTIAL SAR INTERFEROMETRY

Andreas Benedikter, Marc Rodriguez-Cassola, Pau Prats-Iraola, Kristina Belinska, Gerhard Krieger

Microwaves and Radar Institute, German Aerospace Center (DLR)

ABSTRACT

Plenty of data records demonstrate that differential InSAR acquisitions of snow covered areas are often affected by severe temporal decorrelation, complicating the estimation of snow physical parameters such as the snow water equivalent. The decorrelation effect is commonly attributed to a change in the underlying scattering center distribution due to melting/refreezing, compacting of snow, or redistribution of underlying vegetation. We demonstrate that a mere change of the dielectric constant of a dry snow cover may lead to severe decorrelation, even without a change in scatterer distribution, which provides additional opportunities for the estimation of snow parameters. In this paper, a first discussion of the snow-induced decorrelation effect is provided and the derived model is evaluated against Sentinel-1 12-day coherence data using SWE measurements provided by the Copernicus Global Land Service.

Index Terms— D-InSAR, SAR interferometry, snow, decorrelation, snow water equivalent

1. INTRODUCTION

The potential of differential SAR interferometry (D-InSAR) to measure snow parameters –in particular, the snow water equivalent (SWE)– has been demonstrated in several studies [1–3]. The concept relies on the penetration capability through snow at microwave frequencies and an almost linear dependence of the D-InSAR phase to a change in snow height and density between the repeat acquisitions. It has been stated in several experiments that temporal decorralation is the main limiting factor in D-InSAR SWE retrieval [1–3]. The decorrelation increases significantly for higher frequencies and longer temporal baselines. Several studies show a fairly good conservation of coherence at L band [3]. At C band and X band, severe decorrelation has been reported, especially for the 12 and 11 day repeat cycle of Sentinel-1 and TanDEM-X, respectively. The decorrelation effect is commonly attributed to a change in the underlying scattering center distribution due to melting/refreezing, snow accumulation, or redistribution of underlying vegetation [1, 2]. Let us assume dry snow conditions during the D-InSAR time interval caused by cold temperatures, where the backscatter contribution from the snow surface and volume can be expected to be much less than the backscatter from the underlying ground (e.g., rock, soil, ice, vegetation), the decorrelation explanation connected to a change in scatterer distribution feels somewhat counter-intuitive, since: i) no melting and refreezing should happen, ii) snow accumulation should not significantly contribute to the backscatter, and iii) the ground scatterer distribution (e.g., vegetation) is rather experiencing a conservation than a redistribution, compared to the snow-free case. Still, strong decorrelation is omnipresent in snow-covered areas at low temperatures.

In this paper, we provide an alternative explanation that does not require a scatterer redistribution. We show that a mere change of the snow permittivity may result in a decorrelation, due to a change of the vertical wavenumbers of the radar waves in the snow. A similar effect has been observed in [4] for the soil moisture case.

2. DECORRELATION EFFECT OF DRY SNOW

When penetrating the snow surface, the higher relative permittivity of snow, $\varepsilon_{\mathrm{r,s}}$, compared to air results in a reduced propagation velocity of the radar signals within the snow pack and, consequently, in refraction at the air-snow interface. Following [1], the additional phase delay introduced by the snow cover can be written as

$$\Delta\Phi_{\mathrm{s}} = \frac{4\cdot\pi}{\lambda_0}\cdot Z_{\mathrm{s}}\cdot\left(\sqrt{\varepsilon_{\mathrm{r,s}}(\rho_{\mathrm{s}}) - \sin^2\theta_i} - \cos\theta_i\right), \quad (1)$$

where λ_0 is the wavelength, Z_{s} is the snow height, $\varepsilon_{\mathrm{r,s}}(\rho_{\mathrm{s}})$ is the density dependent relative permittivity of the snow pack, and θ_i is the incident angle. The relative permittivity of dry snow is mainly a function of the snow density and can be computed as $\varepsilon_{\mathrm{r,s}}(\rho_{\mathrm{s}}) = 1 + 1.5995\cdot\left(\rho_{\mathrm{s}}\cdot\mathrm{cm}^3\,\mathrm{g}^{-1}\right) + 1.861\cdot\left(\rho_{\mathrm{s}}\cdot\mathrm{cm}^3\,\mathrm{g}^{-1}\right)^3$ [2], where ρ_{s} is the snow density in $\mathrm{g\,cm^{-3}}$. The density of dry snow typically ranges from $0.1\,\mathrm{g\,cm^{-3}}$ for freshly fallen snow to $0.4\,\mathrm{g\,cm^{-3}}$ for heavily wind compacted snow, resulting in a relative permittivity from 1.16 to 1.76, respectively. The density of the snow pack commonly increases within days due to self-compaction, additional snow accumulation, or wind-induced compaction. Considering orbital repeat cycles of more than 10 days, it is very likely that the radar

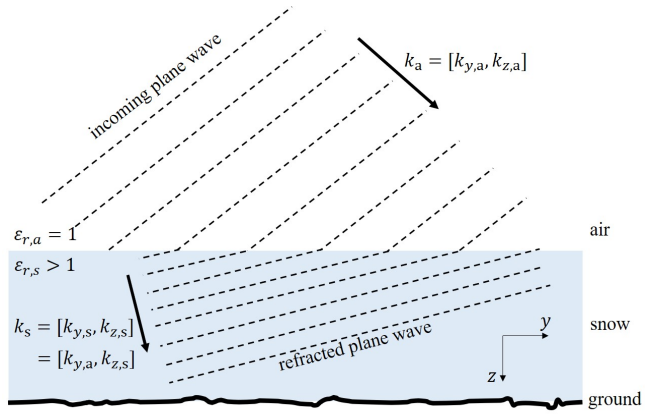

Fig. 1: Plane wave impinging on a smooth snow layer and refracting into the snow volume. Note that only the vertical wavenumber changes when propagating into the snow.

signals of the different SAR acquisitions of the D-InSAR pair will penetrate a snow volume with slightly different permittivity.

From the across-track interferometry case (non-zero baseline) it is well known that a change in the horizontal or vertical wavenumber of the SAR acquisitions with which the ground reflectivity is sampled results in decorrelation of the interferogram [5]. For the D-InSAR case (zero baseline), we note that a change of the wavenumber results from the snow cover above the ground. When observing a plane wave impinging on an air/snow interface, as illustrated in Fig. 1, it is insightful to describe the wave propagation in the wavenumber domain in a decomposed form with a horizontal component, k_y, parallel to the interface and a vertical component, k_z, perpendicular to the interface. According to [5], the wavenumbers in air can be written as $k_{y,\mathrm{a}} = \frac{2\cdot\pi}{\lambda_0}\sin\theta_i$ and $k_{z,\mathrm{a}} = \frac{2\cdot\pi}{\lambda_0}\cos\theta_i$, where θ_i is the incident angle at the air/snow interface. From electromagnetic field theory we know that the horizontal boundary conditions have to be satisfied at the dielectric interface, i.e.,

$$k_{y,\mathrm{a}} = k_{y,\mathrm{s}}, \tag{2}$$

where the indices a and s represent air and snow, respectively. Furthermore, we note that the wave equations must hold in both the air and snow volume (assuming non-magnetic media):

$$k_{y,\mathrm{a}}^2 + k_{z,\mathrm{a}}^2 = \omega^2 \cdot \varepsilon_0 \cdot \mu_0, \tag{3}$$

$$k_{y,\mathrm{s}}^2 + k_{z,\mathrm{s}}^2 = \omega^2 \cdot \varepsilon_{\mathrm{r,s}} \cdot \varepsilon_0 \cdot \mu_0, \tag{4}$$

where ω is the angular frequency and ε_0 and μ_0 are the electric and magnetic constants, respectively. Since the imaginary part of the permittivity of dry snow is negligible at microwave frequencies, (4) can be assumed real valued. From (2), (4) and the expression given in [5] for the horizontal wavenumber, the vertical wavenumber in the snow can be derived as:

$$\begin{aligned} k_{z,\mathrm{s}} &= \sqrt{\omega^2 \cdot \varepsilon_{\mathrm{r,s}} \cdot \varepsilon_0 \cdot \mu_0 - k_{y,\mathrm{a}}^2} \\ &= \frac{2\cdot\pi}{\lambda_0} \cdot \sqrt{\varepsilon_{\mathrm{r,s}} - \sin^2(\theta_i)}. \end{aligned} \tag{5}$$

We can summarize that the horizontal wavenumber is not affected by the snow. However, the vertical wavenumber is altered by the permittivity of the snow. If the scattering centers within one resolution cell are distributed only horizontally, a change in snow permittivity between the two acquisitions of the D-InSAR pair is not causing decorrelation. However, if the scattering centers are also distributed vertically –even just slightly– a change in snow permittivity results in decorrelation. For a vertical backscatter density distribution $f(z)$, if we consider the two images being acquired at two different snow permittivity states, $\varepsilon_{\mathrm{r,s},1}$ and $\varepsilon_{\mathrm{r,s},2}$, the complex coherence can be written as

$$\gamma\left(\varepsilon_{\mathrm{r,s},1}, \varepsilon_{\mathrm{r,s},2}\right) = \frac{\int_0^\infty f(z) \cdot e^{\mathrm{j}2z(k_{z,\mathrm{s},2} - k_{z,\mathrm{s},1})} \mathrm{d}z}{\int_0^\infty f(z) \mathrm{d}z}. \tag{6}$$

In the following, two scattering scenarios are investigated. In the first one, a rough surface underneath the snow cover is assumed where the vertical distribution of the scattering centers is given by a zero-mean normal distribution with a standard deviation (root-mean-square error), σ_z. We have quantified the decorrelation by means of a Monte Carlo simulation. In each iteration, two SAR signals have been simulated

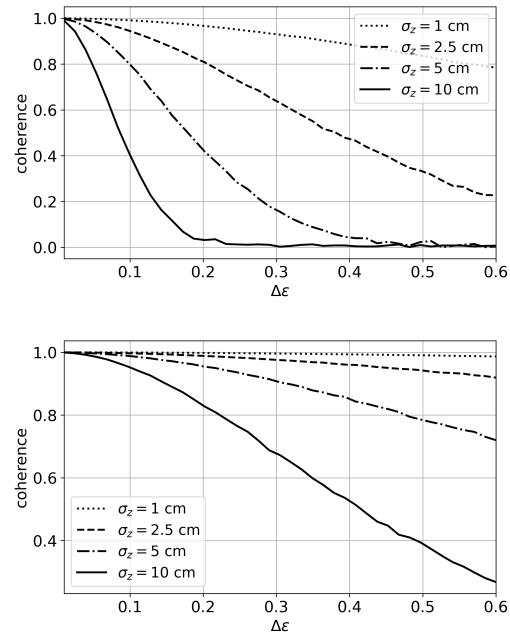

Fig. 2: Simulation of the snow-induced decorrelation effect caused by a change in the permittivity of the snow for different values of relative permittivity difference, $\Delta\varepsilon$, and ground surface roughness σ_z. (Top) C band and (bottom) L band.

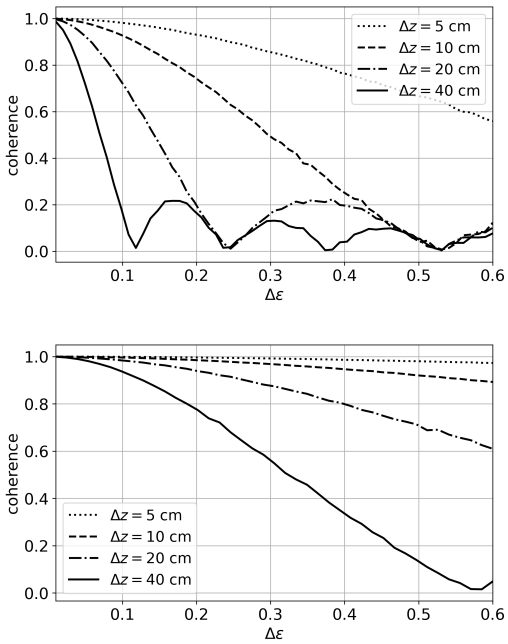

Fig. 3: Simulation of the snow-induced decorrelation effect caused by a change in the permittivity of the snow for different values of relative permittivity difference, $\Delta\varepsilon$, and vertical scattering volume extension Δz underneath the snow cover. (Top) C band and (bottom) L band.

for one realization of scattering center distribution but different relative permittivities, according to the phase delay in (1). In all cases, a zero-baseline scenario has been considered. The mean coherence is then computed over all Monte Carlo iterations. Fig. 2 shows the resulting coherence for different relative permittivity changes, $\Delta\varepsilon$, and different σ_z, where the relative permittivity of the first SAR acquisition is assumed to be 1.2. For the top plot in Fig. 2, a C-band frequency of $5.4\,\mathrm{GHz}$ (Sentinel-1) is used and for the bottom plot an L-band frequency of $1.25\,\mathrm{GHz}$ (NISAR). The decorrelation increases for larger permittivity differences until the coherence drops to zero, i.e, a complete decorrelation of the acquisitions. Also, the decorrelation increases for higher surface roughness, which is in line with the analogy to volume decorrelation in across-track InSAR. The decorrelation is significantly lower in L band. Note that the depth of the snow layer has no influence on the decorrelation.

In a second scattering scenario, a uniform vertical scattering center distribution with a certain vertical extent, Δz, is assumed to be located underneath the snow layer, representing an idealized case of vertically limited volume scattering, e.g., resulting from a vegetation layer. The resulting coherence is shown in Fig. 3 for C and L bands in the upper and lower panel, respectively. Four different uniform volume heights, Δz, are simulated. In contrast to the rough surface scenario, a sinc-like pattern results when evaluating increasing permittivity differences. The sinc-pattern is the Fourier pair to the vertically limited uniform distribution, which results as a consequence of the Fourier transform characteristic of the coherence model in (6). Also here, the analogy to the across-track InSAR case may be drawn, where an increasing permittivity difference corresponds to a larger vertical wavenumber difference (i.e., a larger baseline).

3. SENTINEL-1 DATA ANALYSIS

A validation of the above outlined effect on real D-InSAR data is rather complex since it requires accompanying snow density measurements as well as estimates of the backscatter behavior. Dedicated airborne campaigns or laboratory measurements need to be conducted for the validation of the model. For now, we try to identify evidence for the snow-induced decorrelation in a global Sentinel-1 coherence data set. For a large area in northeast Asia, we use the median 12-day coherence over three months (December, January, February) in Winter 2019/2020 from the global Sentinal-1 coherence data set generated by Kellndorfer et al. [6] with a 3 arcsecond resolution and compare it to an estimate of the median 12-day SWE change ($\Delta\mathrm{SWE}$) in the same time period derived from the *SWE-NH-5km*[1] data of the *Copernicus Global Land Services* based on microwave radiometer measurements. The data are mapped to the same grid and filtered for $\Delta\mathrm{SWE}$ values greater than $4\,\mathrm{mm}$ to ensure that only snow-covered areas are analyzed. The respective maps are shown in Fig. 4. The area under analysis has been chosen because of a high consistency of the *SWE-NH-5km* data in the considered time period. Note that no SWE is mapped over mountains or ice sheets nor in wet snow conditions. Note also that a change in SWE is caused either by a change in snow height, snow density (i.e., permittivity), or both. Snow accumulation commonly results in a snow density change, due to the different properties of freshly fallen and settled snow and the compacting of the older snow layer by the pressure of the new snow layer. Therefore, we assume that in most cases a change in SWE indicates a slight density, i.e., permittivity, change.

Fig. 5 shows the normalized (for each $\Delta\mathrm{SWE}$ bin) 2-D histogram. Coherence values between 0 and 0.75 are visible and a clear correlation between the coherence and the $\Delta\mathrm{SWE}$ can be observed. The coherence falls drastically for increasing $\Delta\mathrm{SWE}$. When looking closely, one can distinguish two patterns in the histogram. One that falls over almost the whole $\Delta\mathrm{SWE}$ extent of the histogram from a coherence value of roughly 0.7 to 0. Besides, in the $\Delta\mathrm{SWE}$ intervals $[12\,\mathrm{mm}, 21\,\mathrm{mm}]$ and $[21\,\mathrm{mm}, 28\,\mathrm{mm}]$ two side lobes of what might be interpreted as a sinc-pattern are visible, where the

[1] The product was generated by the land service of Copernicus, the Earth Observation program of the European Commission. The research leading to the current version of the product has received funding from various European Commission Research and Technical Development programs. The product is based on SWE-NH-5km data ((c) ESA and distributed by FMI).

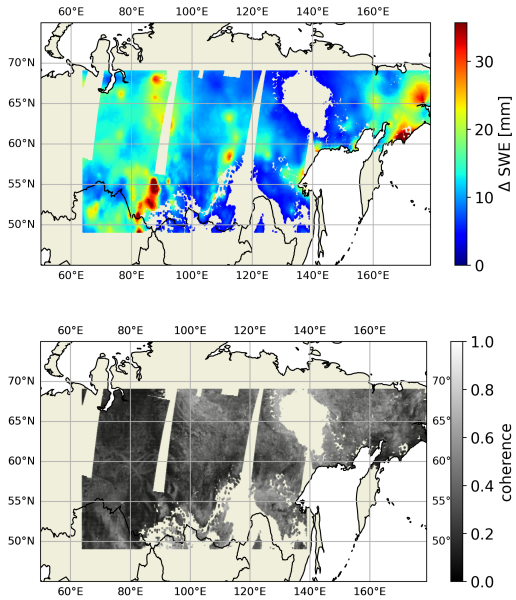

Fig. 4: Maps of median values of ΔSWE (top) and Sentinel-1 12-day coherence (bottom) for a large area in northeast Asia.

main lobe coincides with the first pattern. The two patterns may be attributed to similar scattering scenarios as discussed in the previous section, a rough surface and a volume-like scattering distribution underneath the snow cover. However, no data are available at the moment to proof this assumption and other temporal decorrelation effects, such as temporal changes of the backscatter distribution, might be present in these data. For all these reasons, an inversion of the snow parameters is not attempted in this contribution. Still, the clear correlation between the InSAR coherence and the ΔSWE, together with the similarity of the histogram and the decorrelation patterns shown in Section 2, support that the dry snow decorrelation effect might be a relevant, if not the dominating one.

4. CONCLUSION

We have shown that a permittivity change of a snow layer may result in severe decorrelation of a D-InSAR acquisition if the scattering centers within a resolution cell are not only distributed horizontally, but also vertically, even if just slightly. The decorrelation increases for higher frequencies, a larger change in permittivity, and a larger vertical extent of the backscatter distribution within one resolution cell. We have also shown that this model of snow-induced decorrelation might be compatible with the wide-area analysis of Sentinel-1 12-day coherence data. Further validation with dedicated campaigns might be helpful and will be subject of a future work. The identified correlation between coherence and ΔSWE may allow to exploit the decorrelation effect to invert snow parameters. Furthermore, the described dependence of the vertical wavenumber to the permittivity may be used to generate tomographic information from multiple zero-baseline acquisitions, similar to the virtual bandwidth concept introduced for the soil moisture case in [7].

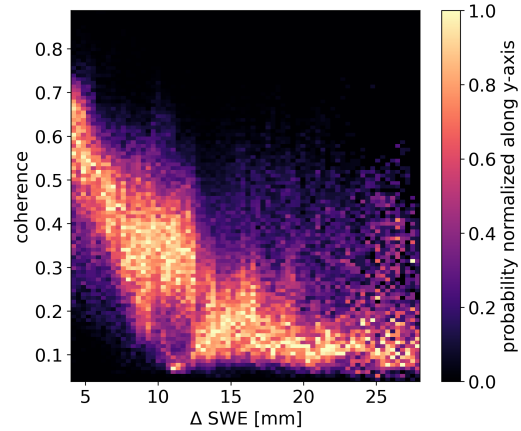

Fig. 5: 2-D histogram relating the maps in Fig. 4, normalized for each ΔSWE bin. Note that the form of the histogram is similar to the patterns shown in the analysis of Section 2.

5. REFERENCES

[1] T. Guneriussen, K.A. Hogda, H. Johnsen, and I. Lauknes, "InSAR for estimation of changes in snow water equivalent of dry snow," *IEEE TGRS*, vol. 39, no. 10, pp. 2101–2108, 2001.

[2] Silvan Leinss, Andreas Wiesmann, Juha Lemmetyinen, and Irena Hajnsek, "Snow water equivalent of dry snow measured by differential interferometry," *IEEE JSTARS*, vol. 8, no. 8, pp. 3773–3790, 2015.

[3] Kristina Belinska, Georg Fischer, and Irena Hajnsek, "Differential SAR interferometry and co-polar phase differences for snow water equivalent estimation," in *EUSAR 2022*, 2022, pp. 1–4.

[4] Francesco De Zan, Alessandro Parizzi, Pau Prats-Iraola, and Paco López-Dekker, "A SAR interferometric model for soil moisture," *IEEE TGRS*, vol. 52, no. 1, pp. 418–425, 2014.

[5] F. Gatelli, A. Monti Guarnieri, F. Parizzi, P. Pasquali, C. Prati, and F. Rocca, "The wavenumber shift in SAR interferometry," *IEEE TGRS*, vol. 32, no. 4, pp. 855–865, 1994.

[6] Josef Kellndorfer et al., "Global seasonal Sentinel-1 interferometric coherence and backscatter data set," *Scientific Data*, vol. 9, no. 1, pp. 73, Mar 2022.

[7] Keith Morrison and John Bennett, "Virtual-bandwidth SAR (VB-SAR) for sub-surface imaging," in *EUSAR 2014*, 2014, pp. 1–4.